

Grain topology in Ti–6Al–4V welds—Monte Carlo simulation and experiments

S Mishra and T DebRoy

Department of Materials Science and Engineering, The Pennsylvania State University, University Park, PA 16802, USA

Received 19 February 2004

Published 14 July 2004

Online at stacks.iop.org/JPhysD/37/2191

doi:10.1088/0022-3727/37/15/022

Abstract

The importance of topological features of grains in the evolution of grain structure is well recognized in isothermal systems. However, during fusion welding, strong spatial gradients of temperature exist in the heat-affected zone (HAZ), and this region undergoes rapid heating and cooling. The effects of spatial and temporal variations of temperature on the topological class distribution, relationship between size and topology of grains and the interdependence between grain topology and its neighbours are not known. Topological features of grains in the HAZ of Ti–6Al–4V alloy welds were measured for various heat inputs in the range 0.55–4.33 MJ m⁻¹. The topological class distributions were also calculated using a three-dimensional Monte Carlo model utilizing thermal cycles computed from a well tested numerical heat transfer and fluid flow model. The computed results showed that the topological class distributions were unaffected by the spatial and temporal variations of temperature. Experimental investigations of a few sections confirmed the simulation results. The average grain size for each edge class varied linearly with the edge class number. The local topological environment, i.e. the average number of sides of neighbours, n_n , varied linearly with the inverse of the number of sides of grains, $1/n_r$, at a given location in the HAZ. Locations with the same topological environment showed the same grain size, indicating the significant influence of grain topology on grain growth in the HAZ.

1. Introduction

The importance of grain topology in the evolution of grain structure during isothermal processing is well recognized in the literature [1–15]. Considering thermodynamic equilibrium, Smith [1] argued that a two-dimensional equilibrium grain structure must consist of six-sided grains. Any deviation from the equilibrium grain structure would lead to grain growth. In a two-dimensional section, the requirement of equilibrium eliminates the vertices at which more than three edges meet [1], causing a four-rayed vertex to decompose into two three-rayed vertices [16], as shown in figure 1.

During fusion welding, significant spatial gradients of temperature exist in the heat-affected zone (HAZ), and this

region undergoes strong thermal cycles involving rapid heating and cooling. Therefore, the results from isothermal studies are not directly applicable for understanding the evolution of grain structure in the HAZ. Mishra and DebRoy [17] have recently explored the effects of spatial and temporal variations of temperature on the average grain size and grain size distributions in the HAZ of Ti–6Al–4V alloy during gas tungsten arc (GTA) welding for various welding conditions. This alloy is widely used in aerospace applications. In the work of Mishra and DebRoy [17], the evolution of grain topology, which is an important feature in understanding the grain structure evolution in the HAZ of the alloy, was not addressed and answers to many important questions related to grain topology are not known. For example, how does the

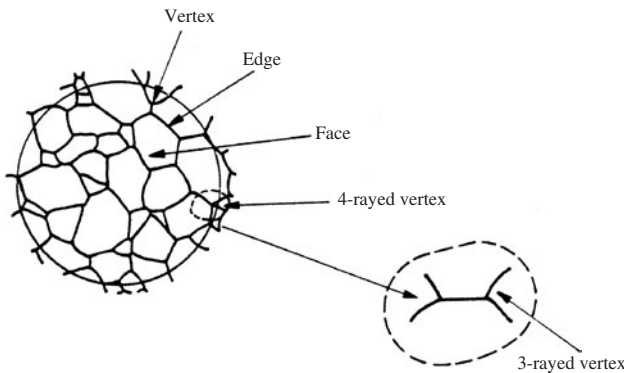


Figure 1. Typical two-dimensional section through a three-dimensional grain structure. The four-rayed vertex tends to decompose into two three-rayed vertices as grain growth occurs [16].

thermal cycle affect the topological class distribution? How important is the spatial gradient of temperature? Are the size and topology of grains related in the HAZ? How is the topology of a grain related to that of its neighbours in the HAZ? This paper explores the answers to the above questions, both experimentally and theoretically.

2. Experimental procedure and mathematical modelling

The details of the experimental procedures are given in [17]. In short, GTA welds were made on extra low interstitial (ELI) grade Ti-6Al-4V alloy samples. Optical metallography was performed on post-weld samples. Characterization of topological features of prior-beta (β) grains in the HAZ of post-weld Ti-6Al-4V alloy samples using computer assisted techniques was difficult because of the impingement of a basket-weave acicular $\alpha + \beta$ on the grain boundaries during cooling [18]. Therefore, the topological features were determined manually. The number of sides and size of individual grains were measured on planar sections at different locations in the HAZ.

The topological features of grains, i.e. the number of sides of individual grains and the number of sides of their neighbours, were calculated at different locations in the HAZ from the grain structure map as described in [17]. In short, the procedure involved modelling of heat transfer and fluid flow [17, 19–30] in the weldment in three dimensions and, utilizing the computed temperature profiles, simulation of the grain structure evolution using the Monte Carlo (MC) technique. The MC technique has been found to be reliable for the simulation of grain growth in the HAZ as indicated in the recent literature [17, 19, 30–33] and references cited therein.

3. Results and discussion

3.1. Topological class distribution under different thermal cycles and same temperature gradient

The changes in the grain structure are affected by both the temperature gradient and the thermal cycles [17]. In order to separate the effects of these two factors and understand the effect of thermal cycles on the topological class distribution,

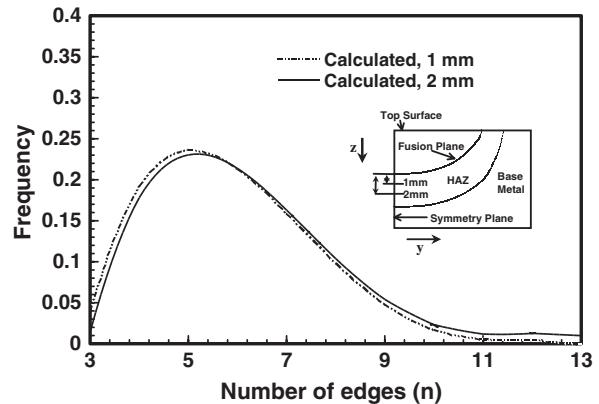


Figure 2. Calculated topological class distributions at two monitoring locations in the HAZ that experience the same temperature gradient but different thermal cycles. The distributions are for locations 1 and 2 mm from the fusion plane on the mid-section vertical symmetry plane for a heat input of 4.33 MJ m^{-1} . Since an area is needed to determine the grain structure and topological features, results from a strip $\pm 250 \mu\text{m}$ on either side of the monitoring location were used.

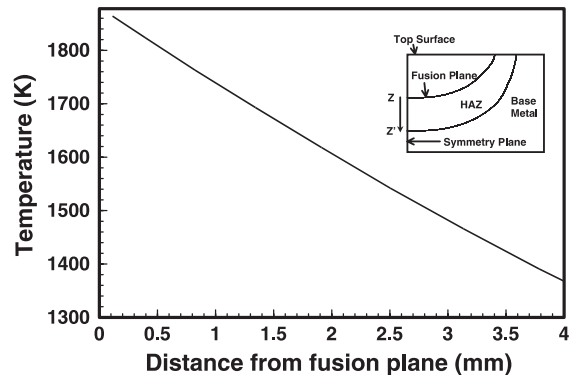


Figure 3. Variation of peak temperature with distance from the fusion plane (along ZZ') on the mid-section vertical symmetry plane for a heat input of 4.33 MJ m^{-1} .

two locations were selected where the thermal cycles were significantly different but the dominant temperature gradients were the same. The topological class distribution, i.e. the proportion of grains having a specific number of sides (frequency) versus the number of sides, is plotted in figure 2 for these monitoring locations. At both locations, the main temperature gradient was in the downward (z) direction. As shown in figure 3, the z -direction temperature gradients were the same at both the locations. Temperature gradients along the direction perpendicular to the welding direction on the horizontal plane, i.e. along the y -direction, were zero because both monitoring locations were on the mid-section vertical symmetry plane. The temperature gradients along the welding direction (x) were negligible directly under the heat source at both these locations. Figure 4 shows that the thermal cycles at the two monitoring locations were significantly different. Since the topological class distributions were the same at both the locations (figure 2), it can be concluded that the changes in the thermal cycles did not affect the topological class distributions. Furthermore, the topological class distributions show the same attributes as those observed during normal grain growth under isothermal conditions. The thermal cycles have

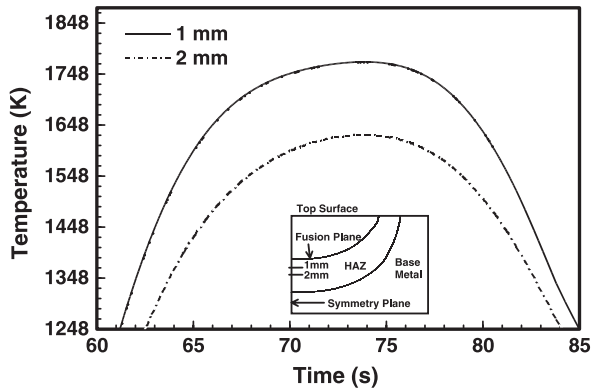


Figure 4. Computed temperature fields at distances of 1 and 2 mm from the fusion plane on the mid-section vertical symmetry plane for a heat input of 4.33 MJ m^{-1} . The timescale is calculated by dividing the x -distance by the welding speed, and time = 0 is arbitrarily set when the heat source is located at $x = 0$.

the same effect on the topological class distribution as the collective effect of many small isothermal steps.

The distribution is characterized by the frequency increasing rapidly for a small number of grain edges and decreasing gradually when the number of edges exceeds six. The average edges per grain are approximately equal to six. This value is consistent with the general topological rule [1, 6, 8, 34], i.e. the average number of sides of grains in a domain, $\langle n \rangle$, is equal to six and grains with less than six sides tend to shrink and those with more than six sides tend to grow. Thus, it can be concluded that this rule is also followed in the HAZ where the grain growth occurs under steep temperature gradients.

3.2. Topological class distribution under different temperature gradients but same thermal cycle

In order to understand the effect of a temperature gradient on the topological class distribution, two systems were considered, both undergoing the same thermal cycle but one with a significant spatial gradient of temperature and the other without it. Calculations of grain growth in the HAZ of the Ti-6Al-4V weldment considered both spatial and temporal variations of temperature. Another calculation considered a three-dimensional specimen that was subjected to the same thermal cycle at all locations. Thus, there was no spatial variation of temperature due to the bulk heating of this specimen, although the temperatures at all locations did vary significantly with time. The thermal cycle used for bulk heating was the same as that observed at the monitoring location in the HAZ. The topological class distribution at a monitoring location in the HAZ is compared with that under bulk heating conditions in figure 5. The similarity of the two topological class distributions indicates that the distribution is unaffected by the temperature gradient.

3.3. Effect of alloy composition on the topological class distribution

In order to examine the effect of the alloying elements on the topological class distribution, the topological class

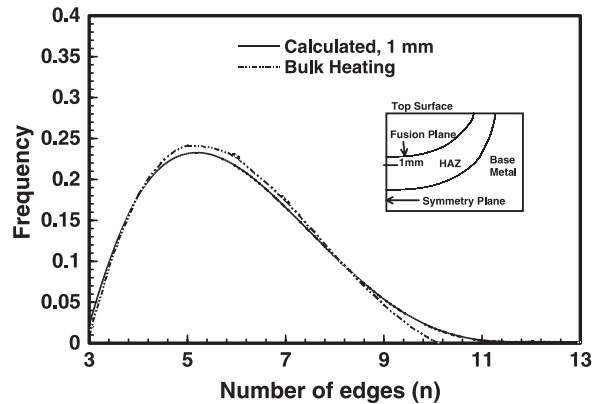


Figure 5. Calculated topological class distributions for two systems, both undergoing the same thermal cycle but different temperature gradients. One distribution is for a monitoring location 1 mm from the fusion plane in the HAZ on the mid-section vertical symmetry plane for a heat input of 2.13 MJ m^{-1} . The temperature gradient at this location is 164 K mm^{-1} , and the peak temperature of the thermal cycle is 1714 K. The other distribution corresponds to a situation where the entire calculation domain was subjected to the same thermal cycle as that experienced at the monitoring location in the HAZ.

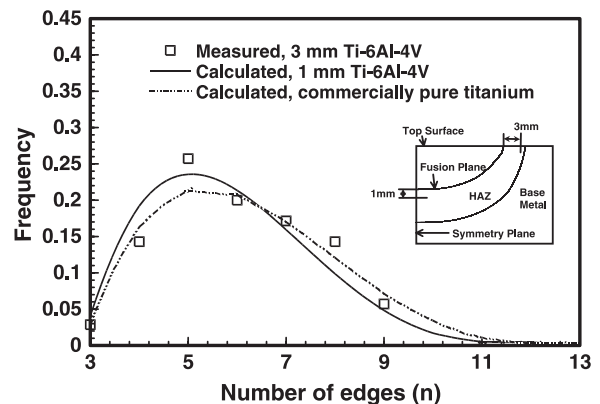


Figure 6. Experimental and calculated topological class distributions at different locations in the HAZ of a Ti-6Al-4V alloy weld for a heat input of 4.33 MJ m^{-1} . The experimental topological class distribution is at 3 mm from the fusion plane on the top surface, where the temperature gradient is 192 K mm^{-1} and the peak temperature of the thermal cycle is 1302 K. The calculated distribution is at 1 mm from the fusion plane on the mid-section vertical symmetry plane, for which the temperature gradient and thermal cycle are given in figures 3 and 4, respectively. The solid line shows the calculated topological class distribution in the HAZ of a commercially pure titanium weld at 2.5 mm from the fusion plane on the top surface for a heat input of 2.0 MJ m^{-1} [33].

distribution in the HAZ of commercially pure titanium [33] is compared with that in the HAZ of Ti-6Al-4V alloy in figure 6. The similarity of the distributions indicates that the topological class distribution is unaffected by the concentration of alloying elements in titanium. Furthermore, good agreement between the experimental and the calculated topological class distributions in figure 6 indicates the reliability of the calculated results and supports the earlier arguments that locations experiencing different temperature gradients and thermal cycles show the same topological class distribution. The topological class distribution in both specimens is characteristic of isothermal grain growth [4, 5]

in metals and alloys. The topological class distribution is influenced by the space filling requirements and is independent of the material composition.

3.4. Relation between average grain size and number of edges

In order to understand the relation between the average grain size and the number of edges, the average grain size for each edge class is plotted against the edge class number (number of sides) in figures 7 and 8. The monitoring locations experienced different thermal cycles and different temperature gradients. A linear relationship between the edge class and the average grain size is observed in all the cases. The grains with a larger number of sides, having a lower grain boundary length per unit area, are larger in size. This observation is consistent with the argument made by Smith [1] that grain growth is accompanied by reduction in grain boundary length

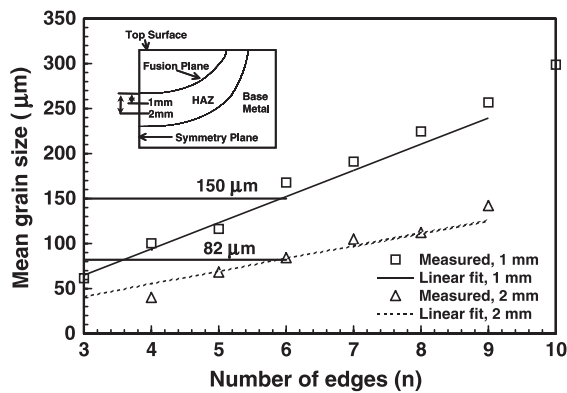


Figure 7. Mean grain size versus number of edges at distances of 1 and 2 mm from the fusion plane on the mid-section vertical symmetry plane for a heat input of 1.10 MJ m^{-1} . The symbols represent the experimental data, while the lines are the linear fit to the calculated results. The temperature gradient at the two locations is 197 K mm^{-1} , and the peak temperature of the thermal cycle for the 1 mm location is 1681 K and that for the 2 mm location is 1484 K .

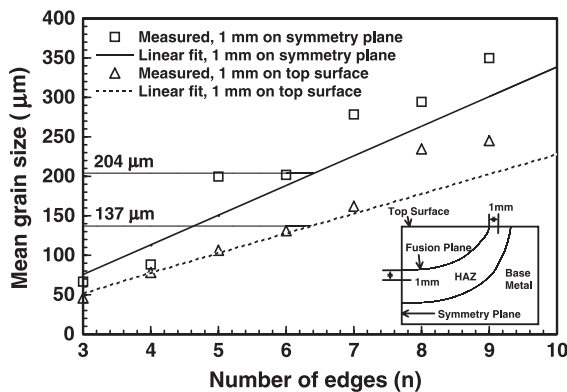


Figure 8. Mean grain size versus number of edges at 1 mm from the fusion plane on the top surface and the mid-section vertical symmetry plane for a heat input of 2.13 MJ m^{-1} . The symbols represent the experimental data, while the lines are the linear fit to the calculated results. For the top surface location the temperature gradient is 231 K mm^{-1} and the peak temperature of the thermal cycle is 1647 K . For the mid-section vertical symmetry plane location the temperature gradient is 164 K mm^{-1} and the peak temperature of the thermal cycle is 1714 K .

per unit area. The calculated results slightly underestimate the measurements in figure 8, for grains with a large number of sides. A contributing factor in the difference between the experimental results and the computed values is the difficulty in accommodating many large grains in a small area of monitoring section. On the whole, fair agreement is observed between the calculated and the experimental results, indicating that the MC model can adequately predict the relationship between the size and topology of grains in the HAZ. The horizontal lines in figures 7 and 8 represent the average grain size at the respective locations. It is observed that the average grain size corresponds to grains with approximately six sides, which is the average number of sides of grains at any location.

3.5. Relationship with the topology of neighbouring grains

Figure 9 explores the effect of the local topological environment on grain growth in the HAZ. The average number of sides of neighbouring grains, n_n , is plotted against the inverse of the number of sides of grains, $1/n_r$, in figure 9. A linear relationship is observed. This relation is consistent with an important relation for the topology of neighbouring grains discovered by Aboav [11, 12] for isothermal grain growth in polycrystalline magnesium oxide. Isothermal studies on iron [4, 5] also revealed a similar relation. It is noteworthy that grain growth under a spatial gradient of temperature, as in the HAZ, also follows this relationship. This relationship defines the local topological environment at a given location in the HAZ such that the grains with fewer sides, for example three, have on an average more than eight-sided neighbours. No cluster was found with all fewer than six-sided or all larger than six-sided grains at a given location. Thus, the topological environment in the HAZ allows for grain growth with the shrinkage of grains with less than six sides. Figure 9 contains plots for two locations, i.e. 1 mm from the fusion plane on the top surface and 2 mm from the fusion plane on the mid-section vertical symmetry plane. The plots overlap each other, showing that the local topological

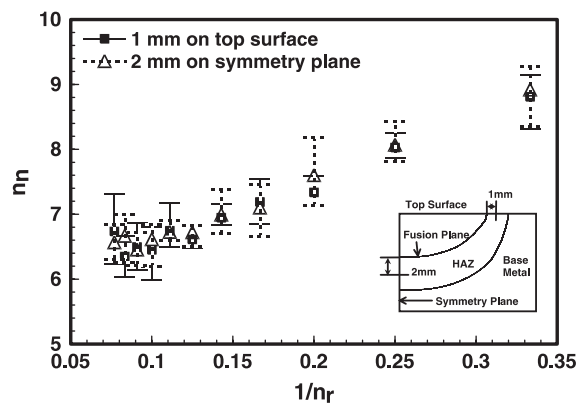


Figure 9. Computed average number of sides of neighbours (n_n) versus the inverse of the sides of grains ($1/n_r$) at 1 mm from the fusion plane on the top surface and 2 mm from the fusion plane on the mid-section vertical symmetry plane. Both the results are for a heat input of 2.13 MJ m^{-1} . At the top surface location the temperature gradient is 231 K mm^{-1} and the peak temperature of the thermal cycle is 1647 K . At the mid-section vertical symmetry plane location the temperature gradient is 164 K mm^{-1} and the peak temperature of the thermal cycle is 1550 K .

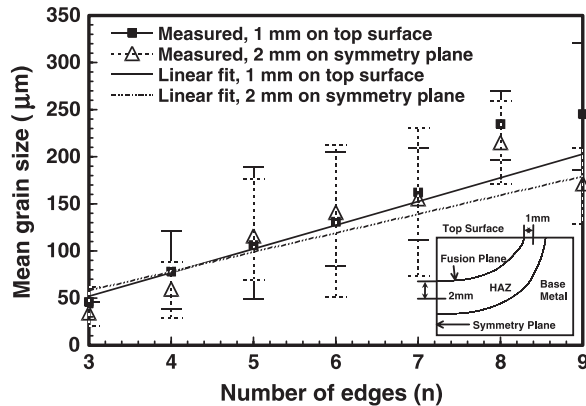


Figure 10. Experimentally measured mean grain size versus number of edges at 1 mm from the fusion plane on the top surface and 2 mm from the fusion plane on the mid-section vertical symmetry plane. The lines represent the linear fit to the calculated results. Both the results are for a heat input of 2.13 MJ m^{-1} . At the top surface location the temperature gradient is 231 K mm^{-1} and the peak temperature of the thermal cycle is 1647 K . At the mid-section vertical symmetry plane location the temperature gradient is 164 K mm^{-1} and the peak temperature of the thermal cycle is 1550 K .

environment at these locations is almost identical. Since the grain topology plays a major role in grain growth, a similar grain size versus grain topology relation should be expected at both locations. This can be clearly observed in figure 10, which shows the experimental plots of average grain size for each edge class versus the edge class number at the two locations considered. The two plots are almost identical, showing the impact of topological properties on grain growth in the HAZ. Furthermore, the results indicate the ability of the MC model to predict accurately these relationships.

4. Conclusions

The topological features of grains in the HAZ of Ti-6Al-4V alloy GTA welds were studied experimentally and theoretically using a three-dimensional MC model. The following are the main conclusions:

1. The computed topological class distributions at two locations subjected to different thermal cycles but the same temperature gradient were identical. The distributions were unaffected by the intensity of thermal cycles. Experimental investigation of a few cuts confirmed the calculated results. The distributions resembled those observed under normal isothermal grain growth in metals and alloys.
2. The topological class distributions in two specimens subjected to the same thermal cycles, one with a significant temperature gradient and the other without it, showed the same topological class distribution. The distribution was unaffected by the temperature gradient.
3. The topological class distributions in the HAZ of the Ti-6Al-4V alloy agreed well with those for commercially pure titanium, indicating that the distributions are not affected by the additions of alloying elements.
4. The average grain size for each edge class varied linearly with the edge class number, i.e. number of sides, at different locations in the HAZ. The grains with a greater number of sides were larger. Grains of average size had six sides.
5. The calculated results showed a linear relation between the average number of sides of neighbours and the number of sides of grains at various locations in the HAZ. This result demonstrates the importance of the local topological environment in the normal grain growth even under strong thermal cycles and temperature gradients.

Acknowledgments

This research was supported by a grant from the US Department of Energy, Office of Basic Energy Sciences, Division of Materials Sciences, under grant number DE-FGO2-01ER45900. The authors thank Drs Todd A Palmer and John W Elmer of LLNL for providing welded samples and for their interest in the research. The authors thank Mr Wei Zhang, Mrs Xiuli He, Mr Amit Kumar and Dr Amitava De for their comments during the preparation of this manuscript.

References

- [1] Smith C S 1952 *Metal Interfaces* (Ohio: ASM International) p 65
- [2] Srolovitz D J, Anderson M P, Sahni P S and Grest G S 1984 *Acta Metall.* **32** 793
- [3] Saito Y and Enomoto M 1992 *ISIJ Int.* **32** 267
- [4] Sista S and DebRoy T 2001 *Metall. Mater. Trans. B* **32** 1195
- [5] Hu H 1974 *Can. Metal. Q.* **13** 275
- [6] von Neumann J 1952 *Metal Interfaces* (Ohio: ASM International) p 108
- [7] Fradkov V E, Glicksman M E, Palmer M and Rajan K 1994 *Acta Metall. Mater.* **42** 2719
- [8] Mullins W W 1956 *J. Appl. Phys.* **27** 900
- [9] Aboav D A and Langdon T G 1969 *Metallography* **1** 333
- [10] Aboav D A and Langdon T G 1969 *Metallography* **2** 171
- [11] Aboav D A 1980 *Metallography* **13** 43
- [12] Aboav D A 1970 *Metallography* **3** 383
- [13] Glicksman M E, Rajan K, Nordberg J, Palmer M, Marsh S P and Pande C S 1992 *Mater. Sci. Forum* **94-96** 909
- [14] Singh S B and Bhadeshia H K D H 1998 *Mater. Sci. Technol.* (UK) **14** 832
- [15] Wakai F, Enomoto N and Ogawa H 2000 *Acta Mater.* **48** 1297
- [16] Atkinson H V 1988 *Acta Metall.* **36** 469
- [17] Mishra S and DebRoy T 2004 *Acta Mater.* **52** 1183
- [18] Donachie M J Jr 2000 *Titanium: A Technical Guide* 2nd edn (Ohio: ASM International)
- [19] Yang Z, Sista S, Elmer J W and DebRoy T 2000 *Acta Mater.* **48** 4813
- [20] Elmer J W, Palmer T A, Zhang W, Wood B and DebRoy T 2003 *Acta Mater.* **51** 3333
- [21] He X, Fuerschbach P and DebRoy T 2003 *J. Appl. Phys.* **94** 6949
- [22] Kumar A and DebRoy T 2003 *J. Appl. Phys.* **94** 1267
- [23] David S A, Trivedi R, Eshelman M E, Vitek J M, Babu S S, Hong T and DebRoy T 2003 *J. Appl. Phys.* **93** 4885
- [24] Zhang W, Roy G G, Elmer J and DebRoy T 2003 *J. Appl. Phys.* **93** 3022
- [25] He X, Fuerschbach P W and DebRoy T 2003 *J. Phys. D: Appl. Phys.* **36** 1388
- [26] Hong T and DebRoy T 2003 *Metall. Mater. Trans. B* **34** 267

- [27] Mundra K, DebRoy T and Kelkar K 1996 *Numer. Heat Transf.* **29** 115
- [28] Pitscheneder W, DebRoy T, Mundra K and Ebner R 1996 *Weld. J.* **75** 71s
- [29] Zhang W, Elmer J W and DebRoy T 2002 *Mater. Sci. Eng. A* **333** 321
- [30] Yang Z, Elmer J W, Wong J and DebRoy T 2000 *Weld. J.* **79** 97s
- [31] Sista S, Yang Z and DebRoy T 2000 *Metall. Mater. Trans. B* **31** 529
- [32] Gao J, Thompson R G and Cao Y 1996 *Trends in Welding Research* ed H B Smartt *et al* (Ohio: ASM International) p 199
- [33] Yang Z 2000 *PhD Dissertation* Pennsylvania State University, p 236
- [34] Hillert M 1965 *Acta Metall.* **13** 227